Factors Affecting Lithium Adsorption on Clay Minerals

Mohammed Al-Hamad[1], Shamah Al-Harbi[1], Ahmad AlZoukani[1], Shouxiang Mark Ma[2]

[1]SLB, Schlumberger Dhahran Carbonate Research Centre, 31952 Dhahran, Saudi Arabia.
[2]Saudi Aramco, Reservoir Description Division, 31952 Dhahran, Saudi Arabia

Abstract. Identification and sustainable extraction of lithium from diverse geological sources, specifically clay deposits, have become a critical research priority. When lithium is produced from subsurface formation brine, its original source is in rock solids such as clay minerals, i.e., formation brine is the carrier while the rocks are the supplier. This study focuses on experimentally investigating the adsorption of lithium in calcite/clay mixtures using techniques of XRD, FTIR, ICP-OES, wet chemistry analyses, and bench adsorption experiments. The experiments conducted were controlled with a known mix of minerals and brine properties. Results indicate that the presence of calcite complicates the interpretation of exchangeable cation data in samples of mixed minerals of calcite and clay. While the precision of XRD and FTIR tests was limited to detect 1200 ppm lithium, FTIR identified a unique masking effect of illite peaks that serves as a potential diagnostic for lithium adsorption. Furthermore, bench experiments identified illite as the superior adsorbent, achieving an over 45% efficiency despite its relatively lower CEC comparing to montmorillonite. Findings of this study reveals the complex interactions between lithium and clay minerals, and understanding these interactions would allow one to identify and quantify lithium resources more successfully and produce it more effectively through techniques such as leaching.

1 Introduction

Recently, lithium has become a critical element for modern energy storage technologies, particularly in rechargeable batteries for electric vehicles and grid systems. Lithium as an ion is soluble in water, therefore, it can be found in seawater and underground formation water. Although often with low concentrations, lithium in aqueous brines is an important source as it represents the most economical source of lithium recovery; thus, the most host of global lithium supply [1]. In reservoirs, such lithium deposits have occurred by the leaching of surrounding rocks.

Besides in aqueous brines, lithium is commonly found in rock deposits and clay minerals, with each source possessing distinct mineralogical characteristics and extraction challenges [2, 3]. Rock deposits offer the highest lithium concentrations, with lithium occurring primarily in coarse-grained igneous rocks [4].

In the case of clays, lithium is primarily incorporated into the mineral structure through isomorphous substitution or adsorbed on the clay surface [5]. In reservoirs, lithium enrichment in sedimentary and carbonate-clay systems is driven by either surface weathering, diagenetic mineral transformation, and/or direct adsorption from formation brines [6]. The host of lithium in clay minerals is governed by their structural characteristics, their layer charges and their expandability [7]. Depending on the clay type and its characteristics, lithium can be adsorbed on the internal lattice and/or on the external surface sites [8, 9, 10]. It is generally believed that the ability of clay minerals to host lithium is primarily driven by their Cation Exchange Capacity (CEC) [11, 12]. However, recent studies have shown that even clays with low CEC (such as kaolinite) can adsorb significant amounts of lithium. This phenomenon suggests that additional factors beyond CEC are influencing the enrichment process [13, 14]. In such clay types, lithium is often incorporated structurally within the lattice and/or adsorbed on surfaces or within cavities, rather than through ion exchange.

The main objective of this study is to investigate experimentally the geological relations between CEC, clay type and lithium content, to better understanding the adsorption of lithium in calcite-clay mixtures.

2 Materials and Methods

2.1 Clay and Rock Minerals

The commonly occurring three types of clay minerals were considered for this study: montmorillonite, illite and kaolinite, in addition to calcite mineral, all obtained from the Ward Natural Science. Different mixtures of calcite/clay (3, 6, and 9 wt% of clay relative to calcite) and lithium were prepared (Table 1). Samples of calcite/clay powders were homogenized using an XRD MILL McCrone to ensure that the samples have uniform particle size and thus are representative of the mixing, a critical step for measurement data quality [15, 16].

* Corresponding author: mal-hamad@slb.com

2.2 Fluids

Two brines (Table 1) were used in this work to study the adsorption of lithium in clay minerals. Sodium chloride (NaCl) and lithium carbonate (Li_2CO_3) were sourced from Sigma-Aldrich. Using Li_2CO_3, a lithium solution of 1,200 ppm was prepared and used for the adsorption experiments, where 6.39 g of Li_2CO_3 was needed for 1 L of solution. Table 1 summarizes the details of the solid mixture and brine samples.

Table 1. Details of samples of solid mixtures and brines

Solid Mixture	**Clay**	**Calcite**
3%	3 wt%	97 wt%
6%	6 wt%	94 wt%
9%	9 wt%	91 wt%
30%	30 wt%	70 wt%
9% + 0.639 wt% Lithium	9 wt%	91 wt%
Brine	**$NaCl+Li_2CO_3$**	**H_2O**
1200 ppm Lithium	0 g + 6.39 g	993.6 g
1200 ppm Lithium + 50 kppm NaCl	50 g + 6.39 g	950.0 g

2.3 Cation Exchange Capacity (CEC)

There are different ways of characterizing CEC of clay minerals [17]. In this study, the CEC of the prepared solid mixtures (Table 1) was obtained by using the below two methods: the USDA Handbook 60 (i.e., USDA) and the 1994 Soil & Mineral Analysis, Volume III, ISO 11260:1994 (i.e., ISO) methods. by a commercial lab. For the USDA method, the clay samples were:

1.Leached with a sodium (Na+) salt solution (typically 1N neutral ammonium acetate followed by a NaCl solution) to replace all exchangeable cations with Na+ ions.

2.Then, the excess, non-adsorbed sodium solution was washed from the clay sample, by an alcohol solution.

3.The adsorbed sodium was then extracted/displaced and collected using another cation solution containing ammonium ions (NH_4).

4.The concentration of the displaced sodium in the extracted solution is measured using atomic absorption spectroscopy.

5.The amount of displaced sodium is equivalent to the clay's CEC.

For the ISO method, the clay samples were:

1.Saturated with 0.1 mol/L barium chloride $BaCl_2$.

2.The excess non-adsorbed Barium solution is discarded from the clay samples by centrifugation.

3.Then, 30 ml of 0.02 mol/L magnesium sulfate $MgSO_4$ solution was added to the clay cake.

4.The solute was shaken overnight to ensure the precipitation of $BaSO_2$ and the adsorption of Mg2+.

5.The concentration of excess magnesium in this final solution was obtained using Flame Atomic Absorption Spectrometry. The CEC is calculated by subtracting the residual Mg2+ from the total amount of Mg2+ added

2.4 X-Ray Diffraction (XRD)

After proper sample preparation [15, 16] to have particle sizes smaller than 100 microns, XRD tests were conducted using an Olympus BTX III benchtop diffractometer. The instrument operates with cobalt radiation and an iron filter to reduce fluorescence. Scans were performed over a 2Θ range of 5° to 55°, with a step size of 0.05° and integration time of approximately 20 seconds per step. Only small powder quantities are required to perform these tests, typically less than 20 mg.

2.5 Fourier Transform Infrared Spectroscopy (FTIR)

FTIR measurements were conducted using a Bruker VERTEX 70 spectrometer in the mid-IR (5200–450 cm^{-1}) and far-IR (600–270 cm^{-1}) ranges. Each spectrum was obtained by averaging 32 scans, and background spectra were collected using an empty cell before each measurement. The generated spectra were collected and processed using OPUS software.

2.6 Inductively Coupled Plasma- Optical Emission Spectrometry (ICP-OES)

ICP-OES was used to identify and quantify the elemental composition of the water effluents, post interactions with calcite/clay/lithium mixtures. It works by exciting atoms in a high-temperature argon plasma that causes the atoms to emit light at specific wavelengths. The spectrometer detects and measures the emitted light, allowing for the identification and quantification of the elements. It is worth mentioning that like any analytical technique, ICP-OES carries a level of measurement uncertainty, which is largely driven by matrix effects, calibration, and sampling conditions [26]. This is especially relevant for elements like lithium, which is known to be sensitive to ionization interferences in complex matrices. Test procedures for ICP-OES measurements are summarized below:

1. Mixture samples of 30 g of calcite and 9% of the specific clay (montmorillonite, illite, or kaolinite) were prepared for batch adsorption experiments.

2. The prepared mixtures were added to 200 mL of 1,200 ppm lithium brine (Li brine) and to 1,200 ppm lithium + 50,000 ppm NaCl brine (Mix brine), separately.

3. The mixture was stirred at 1,000 RPM for 16 hours, after which the suspension was allowed to settle and the brine effluent was collected for ICP-OES analysis, and the suspended sample was collected for FTIR analysis.

4. The collected brine samples were measured to obtain the differences between the initial and final concentrations of lithium, determining the amount of adsorbed cations.

2.7 Experimental Procedures

Clay/calcite powder samples were prepared by crushing small rock fragments using a Retsch Jaw Crusher BB50, in order to achieve a fineness of powder sample equal to approximately 0.5 mm. The powder was then subjected to milling to an even finer micro scale using a Retsch Oscillating Mixing Mill MM400. The resulting powder was then sieved and collected for particles sizes 63.5 µm and below [15, 16].

The prepared clay/calcite powders were then mixed in varying proportions, with a clay content of 3%, 6%, and 9% by weight relative to calcite (Table 1). The mixture was homogenized using an XRD MILL McCrone to create a homogeneous sample. Large batches of mixtures were prepared, which were then divided into smaller samples for the various tests. Lithium was introduced into the system using lithium carbonate (Li_2CO_3), resembling lithium-bearing minerals commonly encountered in the subsurface. Lithium carbonate (in powder form), at a concentration of 0.639 wt% (mimicking the concentration of 1,200 ppm lithium) was added to the clay/calcite mixtures.

Sub-samples of the clay/calcite mixtures were used for CEC measurements. Other sub-samples (with and without lithium) were sent for XRD, FTIR measurements. Lastly, sub-samples of the 9% clay/calcite mixtures were used for batch adsorption experiments, at ambient conditions. These experiments were conducted by mixing and stirring 30 g of 9% clay/calcite powder with 200 mL of 1200 ppm lithium and 1200 ppm lithium + 50 kppm NaCl brines, separately. The stirring/reaction was run for 16 hours at 1,000 RPM. The suspension was then given a few hours to settle and separate, after which the clear brine effluent was collected for ICP-OES analysis. While the present study was conducted under ambient conditions, the effects of pH and temperature on adsorption performance are acknowledged as critical parameters and will be investigated in future work to extend the applicability of these findings across a wider range of environmental scenarios.

3 Experimental Results

3.1 CEC Measurement Results

3.1.1 Clay minerals

Table 2 and Figure 1 summarize the CEC values of the three clay minerals, measured by the two methods. From Table 2 and as expected, CEC montmorillonite > CEC illite > CEC kaolinite. Figure 1 also indicates that the CEC values obtained by the two methods correlate extremely well, although the ISO CEC is consistently about 15% lower than that of USDA CEC.

Table 2. CEC of the clay minerals

Clay	**CEC** [meq/100g] USDA	**CEC** [meq/100g] ISO	**CEC** [meq/100g] Average
Kaolinite (KAL)	1.9	1.2	1.6
Illite (Ill)	11.0	9.5	10.3
Montmo-rillonite (Mont)	62.0	53.1	57.6

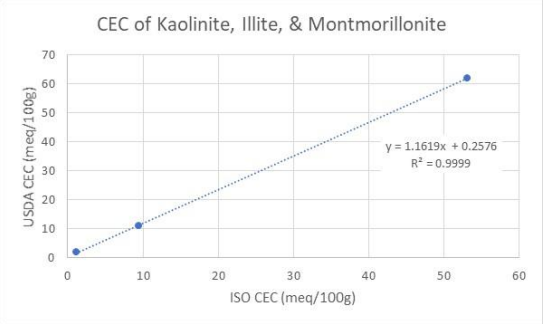

Fig. 1. CEC of clays Kaolinite, Illite, and Montmorillonite, measured by the ISO and USDA methods. CEC values obtained by these two methods agree very well, though the ISO CEC is consistently lower than that USDA CE, by about 15%.

The lower ISO CEC values relative to USAD can be attributed to the different extractants used and the procedures employed by each method. USDA uses a buffered solution (pH 7.0 or 8.2) to measure CEC, while ISO measures CEC on an unbuffered solution [18].

3.1.2 Mixtures of clays and calcite

The above clay CEC measurements tested the suitability of the measurement methodology and equipment. Next, the CEC of the clay/calcite samples, with clay concentrations of 3%, 6%, 9%, and 30%, was measured. Table 3 and Figure 2 summarize the results.

To validate the experimental results, a mixing rule was applied to calculate the total CEC. The calculation (Table 3, last column) treats the Table 2 average results as true CEC values for the pure clays, neglecting the contribution of calcite given its minimal CEC.

$$CEC_{mix} = w_{clay} CEC_{clay} \quad (1)$$

where w_{clay} is the wt% of clay in the solid mixture.

Table 3. CEC of the clay-calcite minerals

Sample	**CEC** USDA	**CEC** ISO	**CEC** Mixing Rule
	[meq/100g]		
3% Kal+97% Cal	14.0	1.3	0.05
6% Kal+94% Cal	13.6	2.3	0.09

9% Kal+91% Cal	20.3	3.7	0.14
30% Kal+70% Cal	26.1		0.47
3% Ill+97% Cal	13.1	1.0	0.31
6% Ill+94% Cal	13.3	1.4	0.62
9% Ill+91% Cal	13.2	1.9	0.92
30% Ill+70% Cal	26.2		3.08
3% Mont+97% Cal	14.7	3.0	1.73
6% Mont+93% Cal	15.6	5.5	3.45
9% Mont+91% Cal	17.9	8.6	5.18
30% Mont+70% Cal	43.3		17.27

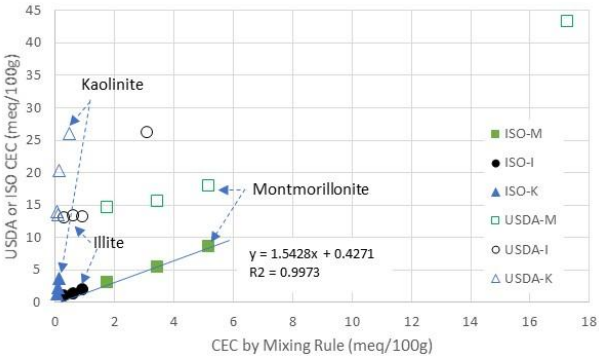

Fig. 2. CEC of clay/calcite mixtures (Table 3).

While the CEC measured by using the ISO method correlates well with mixing rule-based CEC (Eq.1), especially for samples containing illite and montmorillonite, the CEC by the USDA method is abnormally high. As shown in Table 3 and Figure 2 factors beyond clay volume and measurement uncertainty influence the results, especially in low-CEC systems. The presence of calcite interferes with the processes of clay minerals' cation extraction and adsorption. Since both ISO and USDA methods involve the use of an aqueous solution during testing, partial dissolution of calcite could happen which can release calcium ions into the solution. Counting those Ca^{2+} would artificially increase the measured CEC of the mixture, an important reminder when using lab generated core data as hard reference data in engineering and petrophysical applications [19].

3.2 XRD Measurement Results

Mixtures of clay/calcite/lithium carbonate (Li_2CO_3) were analysed by XRD. The first XRD measurement was done on the pure calcite mineral (Figure 3). The acquired spectrum was analysed using a commercial software, Xpowder, where the specific composition of the sample was identified. The result reveals a pure calcite mineralogical composition.

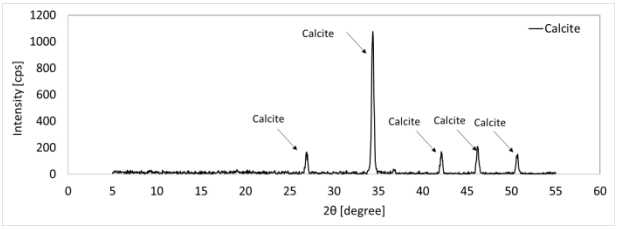

Fig. 3. XRD spectra: pure calcite powder sample

Then, the XRD of a sample of pure lithium carbonate was executed (Figure 4). The spectrum shows multiple sharp and distinct peaks in the mid- to high-angle region, specifically between 25° and 50° 2Θ. These peaks will be used as reference markers for identifying Li_2CO_3 in the calcite/clay/lithium mixture samples. After that, XRD of the calcite/clay mixtures was run, followed by calcite/clay/lithium carbonate mixtures.

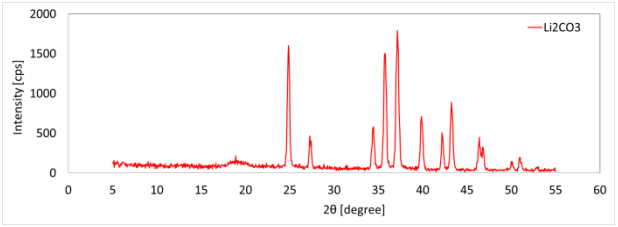

Fig. 4. XRD spectra: Li_2CO_3 powder sample

3.2.1 Kaolinite

XRD of the kaolinite/calcite mixture shows a very strong peak near 34.3° 2Θ, corresponding to calcite (Figure 5). This peak is significantly higher than all others, confirming calcite as the dominant phase in the mixtures. Figure 5 also shows two distinct kaolinite peaks that are highlighted with red dashed boxes. The first peak appears near 14.3° 2Θ, and the second appears near 25° 2Θ, both being specific to kaolinite. These peaks showed a slight increase in intensity as the kaolinite content increases from 3% to 9%, though they remain much lower in intensity compared to the calcite peaks.

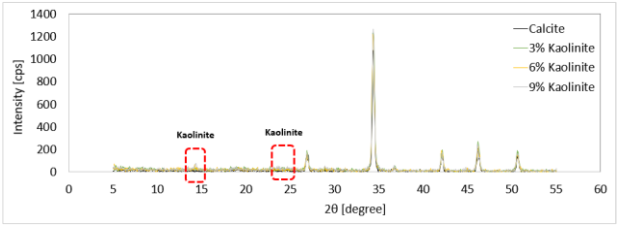

Fig. 5. XRD spectra: samples of calcite mixed with kaolinite at 3%, 6%, and 9% concentrations.

After adding 1200 ppm of Li (from Li_2CO_3) to the 9% kaolinite/calcite mixture, no characteristic signature of Li_2CO_3 was observed in the XRD patterns (Figure 6), indicating that the ppm concentration of lithium carbonate is too low, below the XRD detection limit, typically around 1 to 5 wt% for well-crystallized phases.

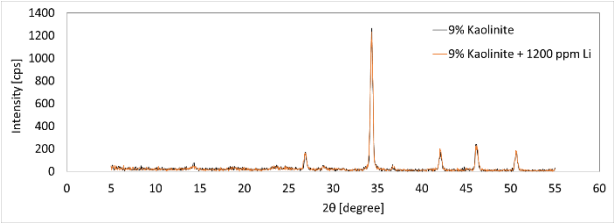

Fig. 6. XRD spectra: mixture of 9% kaolinite/calcite with and without 1200 ppm of Li

3.2.2 Illite

Figure 7 illustrates the 3%, 6%, and 9% illite/calcite mixtures XRD. The spectra showed a distinct peak near 31° 2Θ, characterizing the presence of illite. The peak intensity slightly increases with increasing illite concentration. Despite this trend, the illite signal remains significantly smaller than that of calcite. Here again, the addition of 1,200 ppm of Li salt failed to produce detectable new peaks or alter the existing diffraction profiles of illite/calcite mixtures (Figure 8).

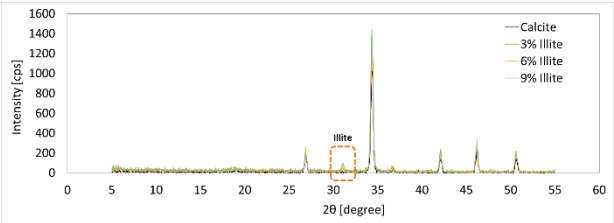

Fig. 7. XRD spectra: mixtures of 3%, 6%, and 9% illite/calcite

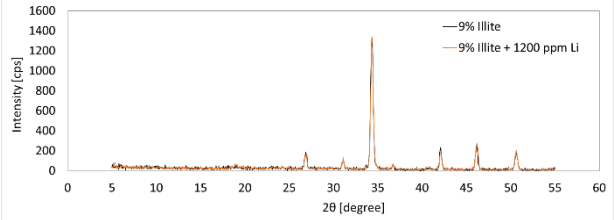

Fig. 8. XRD spectra: mixture of 9% illite/calcite with and without adding 1200 ppm of Li

3.2.3 Montmorillonite

The montmorillonite XRD showed a primary reflection at a significantly lower angle compared to illite and kaolinite. The peak appears more diffuse at 6° and 8° 2Θ (Figure 9). Despite the various concentrations of montmorillonite (3%, 6%, and 9%), the peak intensities remained lower than those of calcite. Furthermore, the data showed no clear trend between montmorillonite concentration and the corresponding peak intensity. Again, no new peaks associated with the addition of 1,200 ppm of Li salt (Figure 10).

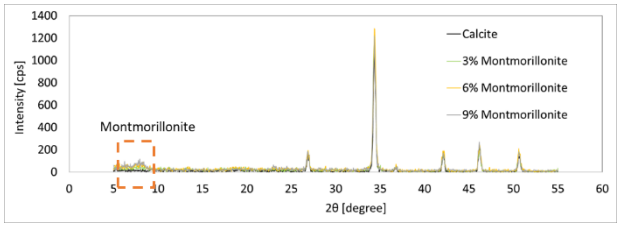

Fig. 9. XRD spectra: mixture of montmorillonite/calcite at 3%, 6%, and 9% of montmorillonite concentrations

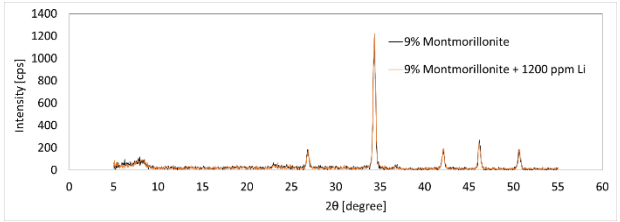

Fig. 10. XRD spectra: mixture of 9% montmorillonite/calcite with and without 1200 ppm of Li

In general, the XRD analysis identifies the calcite and three clay minerals—kaolinite, illite, and montmorillonite peaks at their respective 2Θ angles. While the clays were identified, their peak intensities were significantly lower than that of calcite, due to the much lower concentration of clay in the samples than that of calcite. Although pure lithium carbonate may exhibit distinct diffraction peaks, the addition of 1,200 ppm (0.12 wt%) did not result in any visible lithium effect, mostly because this concentration is below the XRD detection threshold.

3.3 FTIR Measurement Results

Infrared radiation transparent Potassium Bromide (KBr) was used to prepare the FTIR pellets for the mixtures of clay/calcite (kaolinite, illite, and montmorillonite) and lithium salt. A 1:9 sample-to-KBr ratio (0.02 g sample to 0.18 g KBr) was utilized to prepare the pellets. The mixtures were pressed hydraulically into transparent discs for FTIR measurement. The first pellet was prepared for a pure calcite sample (Figure 11 black curve). The FTIR spectrum is dominated by signals arising from the carbonate ions (CO_3^{2-}) present in its structure. As shown in the spectrum, the most prominent peak appears at approximately 1400 cm^{-1}, corresponding to the asymmetric stretching vibration of the carbonate group. Additional characteristic bands are observed around 875 cm^{-1} for the out-of-plane bending vibration and at approximately 712 cm^{-1} for the in-plane bending mode. A broader absorption band appears in the region around 3400 cm^{-1}, which is attributed to moisture absorbed by the hygroscopic KBr used in pellet preparation. The presence of these CO_3^{2-} related vibrational bands in the infrared spectrum confirms the identity of pure calcite.

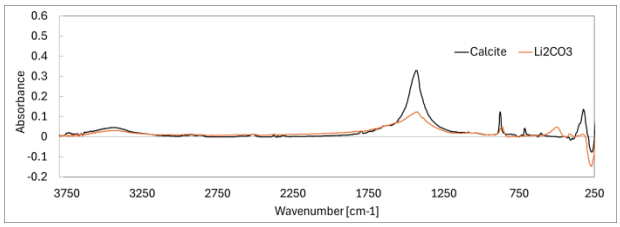

Fig. 11. FTIR Spectra of calcite and lithium carbonate

Then, an FTIR pellet of pure lithium carbonate was prepared and analysed. The spectra (Figure 11 orange curve) showed that the FTIR spectra of calcite and lithium carbonate overlap significantly because they share the same carbonate functional group, making it difficult to identify lithium in a mineralogically mixed sample.

FTIR pellets of the clay/calcite/lithium mixtures were prepared and measured. Since the variations in clay concentration (from 3-9%) did not result in a significant difference in peak intensity from the XRD measurements, we chose to focus only on the 9% clay concentration for the FTIR experiments.

3.3.1 Kaolinite

The kaolinite/calcite sample spectrum exhibits the characteristic peaks of the hydroxyl stretching region at approximately (3695-3620 cm^{-1}), which correspond to different inner-surface hydroxyl groups in the kaolinite structure (Figure 12). Also, new signals, attributed to the Si-O stretching and the Al-OH bonds appear in the 900-1200 cm^{-1} region. The appearance of a sharp peak near 1200 cm^{-1} confirms the incorporation of kaolinite into the calcite matrix.

Similarly, adding 1,200 ppm of lithium salts to the 9% kaolinite/calcite mixture did not result in a new measurable peak, neither did it change the spectra, suggesting that either the lithium is not bonding or interacting with the kaolinite/calcite minerals, or that its peaks are overlapping with the kaolinite/calcite mixture, especially at the low concentration of 1,200 ppm.

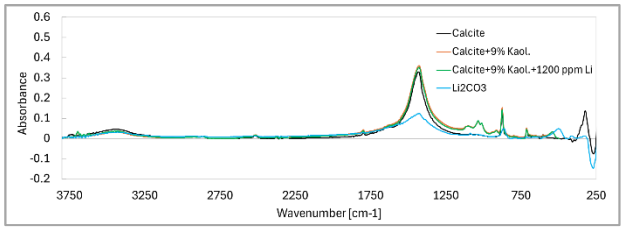

Fig. 12. FTIR Spectra: kaolinite/calcite/lithium mixtures

3.3.2 Illite

Figure 13 presents the FTIR spectra of the illite/calcite sample. A clear absorption band characteristic of illite was observed relative to the calcite background, observed at wavenumbers 470, 530-550 and 1200–900 cm^{-1}. These are assigned to the asymmetric Si–O and Al–O–Si stretching and binding vibrations of illite.

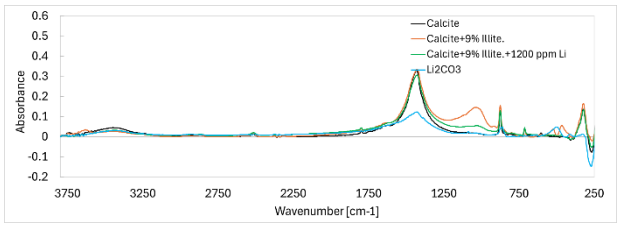

Fig. 13. FTIR Spectra: calcite/illite/lithium mixtures

The presence of 1,200 ppm Li salts in the sample masked the absorbance peaks at 470 cm^{-1}, 530-550 cm^{-1} and 1200–900 cm^{-1}, indicating a possible interaction with the mineral structure rather than remaining chemically isolated. The significance of this observation may lead to further development of using FTIR to detect and quantify lithium in rocks containing illite clay.

3.3.3 Montmorillonite

Figure 14 shows FTIR spectra of the montmorillonite/calcite mixture. The only distinguishable sign of montmorillonite is observed at 1030 cm^{-1}, which is assigned to asymmetric of Si–O stretching. Despite its presence, the intensity of this band remains significantly lower than the dominant calcite absorbance. Moreover, adding lithium salts at 1,200 ppm to the 9% montmorillonite/calcite mixture did not result in a new peak or change to the spectra of the mixture sample. Any Li related effect might be overlapping with that of the solid mixture, making it impossible to recognize the peaks associated with adding this element.

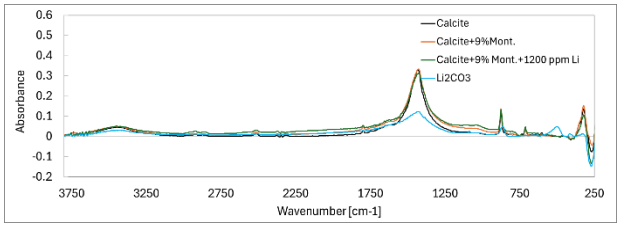

Fig. 14. FTIR Spectra: montmorillonite/calcite/lithium mixtures

In summary, generally, the FTIR analysis identifies the clay minerals of the clay/calcite mixture samples, especially kaolinite and illite. While the clays were identified, their peak intensities were significantly lower than calcite due to the much higher concentration of calcite. Addition of lithium did not produce independent peaks but was observed to mask the existing illite peaks. This masking effect is likely due to the high surface charge of illite [22], which promotes cation adsorption and can influence the intensity of illite related absorption bands. This behaviour is not unique to lithium: other cations such as potassium (K^{+}), calcium (Ca^{2+}), and magnesium (Mg^{2+}) also exhibit similar adsorption and peak-masking effects (Figure 15). Separating lithium from these other cations demands further studies.

It is noted that this masking effect was not observed in samples containing kaolinite or montmorillonite, which could be due to their distinct structural and adsorption properties. For kaolinite, its low adsorption of lithium might be due to a non-expandable structural stability,

which creates a low surface area and minimal CEC [23]. For montmorillonite, with its high adsorption capacity, cations may tend to migrate to the internal structure of the clay, rather than accumulate at the outer surface [24]. As a result, lithium absorption with montmorillonite is less likely to influence surface sensitive FTIR band intensities, and no masking of characteristic montmorillonite absorption features was observed. These findings will be further investigated and discussed in the next section with ICP-OES experimental results.

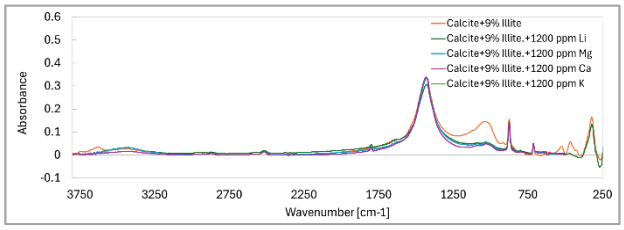

Fig. 15. FTIR Spectra: calcite/illite mixtures with various cations

3.4 ICP-OES Measurement Results

The first ICP-OES experiments were run on the native brines (Li brine and Mix brine). The measured Li concentration was 1, 400 ppm for the known 1,200 ppm Li brine, a measurement uncertainty of 17%. For the Mix brine, the measured Li concentration is essentially the same as the known value of 1,200 ppm, while the Na concentration is slightly lower, 18,800 ppm compared to 19.700 ppm, uncertainty of 5% (Table 4).

Table 4. Summarises the ICP-OES results.

Sample		Ion [kppm]		Measured Ion [kppm]			
		Li	Na	Li	Al	K	Na
Li brine	Brine	1.2	0	1.4	0	0	0
	9% kal	1.2	0	1.4	0.01	0	0
	9% ill	1.2	0	0.6	0.01	12.8	0
	9% Mont	1.2	0	1.4	0	0	0
Mix brine	Brine	1.2	19.7	1.2	0	0	18.8
	9% kal	1.2	19.7	1.4	0.01	0	19.0
	9% ill	1.2	19.7	1.5	0	38.9	18.8
	9% Mont	1.2	19.7	1.4	0	0	19.0

In the case of interactions with 1,200 ppm lithium brine, the ICP-OES analysis showed a distinct adsorption behaviour among the three clay minerals, with illite demonstrating the highest adsorption of lithium ions (>45%), along with the release of native-cations, mainly Potassium (K) and minor Aluminium (Al) as summarized in Table 4. As for kaolinite and montmorillonite, post-reaction analysis did not show measurable changes in lithium concentration, as well as that of Al, K, and Na.

To confirm these observations, the solid mixtures were collected from the suspension following interaction with the brines, dried, and prepared for FTIR analysis. The results for both Li and Mix brines indicate that illite exhibits the highest lithium adsorption, confirmed by the attenuation and masking of its primary characteristic absorption bands (Figure 16). In contrast, montmorillonite and kaolinite, at the studied experimental conditions, showed no significant deviations from their baseline measurements. These may suggest that it would be valuable to further study into clay's adsorption kinetics to characterize the specific Li-binding mechanisms, that differentiate illite performance from the other clays.

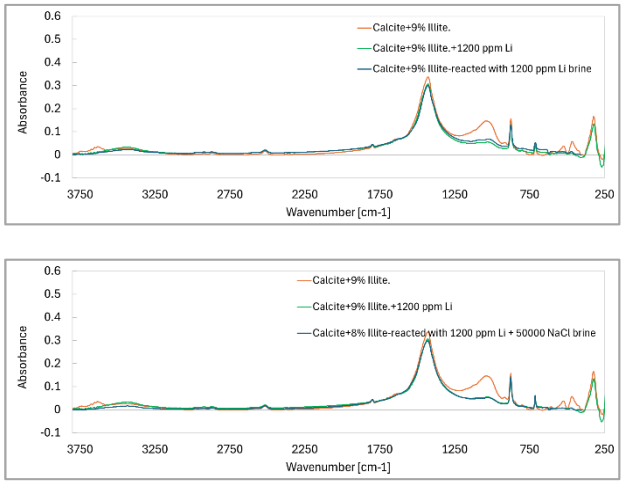

Fig. 16. FTIR Spectra: illite/calcite after interacting with Li and Mix brines.

4 Conclusions

In this study, CEC, XRD, FTIR and ICP-OES tests were conducted and integrated for the purpose of investigating lithium-clay interactions and adsorption.

For clay minerals, the measured CEC by both USDA and ISO methods agreed extremely well, although values by the USDA method are about 16% higher.

For the mixtures of clays and calcite, the measured CEC values, especially the ones using the USDA method, are significantly higher than those predicted by the mixing rule. When comparing the measured vs predicted values, the behaviour of the kaolinite samples is distinctly different from that of illite and montmorillonite samples. For the illite and montmorillonite samples, the measured values by the ISO method correlate well with the predicted values, though were still about 50% higher.

Distinguishing lithium from the host matrix of clays/calcite via FTIR and XRD tests seems challenging, especially at low ppm lithium concentrations, i.e., 1200 ppm. However, the FTIR spectra showed a unique masking effect of lithium adsorption to the illite peaks, which was not observed with montmorillonite and kaolinite. This may need to be further studied for potential use in lithium characterization, after possibly correcting a similar effect of other cations.

From the bench adsorption tests, illite was identified as the most effective adsorbent for lithium, achieving >45% adsorption. This seems to be driven by illite's high surface charge rather than its CEC.

The findings of this study illustrate the challenges of trying to use conventional rock and fluid analysing techniques for ppm level lithium characterisation in rocks and water. Future research may address the masking effect of the illite FTIR results, using advance

characterization techniques such as SEM or X-ray Photoelectron Spectroscopy to perform depth profiling and identify lithium adsorption, either at the clay surface and/or within its internal structure.

5 Acknowledgments

The authors gratefully acknowledge Wael Abdallah and Olivier Sindt for initiating this study and for their technical contributions, which were vital to its success.

6 Nomenclature

CEC: Cation Exchange Capacity
FTIR: Fourier Transform Infrared Spectroscopy
ICP-OES: Inductively Coupled Plasma Optical Emission Spectrometry
XRD: X-ray diffraction

7 References

1. H. C. Starkey. The role of clays in fixing lithium, U.S. Geological Survey Bulletin 1278-F, 11 p. (1982)
2. Bradley, D., Munk, L., Jochens, H., Hynek, S., Labay, K. A preliminary deposit model for lithium brines: U.S. Geological Survey Open-File Report 2013–1006, 6 p. (2013)
3. T. Pan, J. Chen, M.-Y. He, C. Ding, Y. Ma, H. Liang, T. Zhang, and X. Du. Characterization and Resource Potential of Li in the Clay Minerals of Mahai Salt Lake in the Qaidam Basin, China, Sustainability, v. 15, no. 19, 14067 (2023)
4. M.L. Vera, W.R. Torres, C.I. Galli, et al. Environmental impact of direct lithium extraction from brines, Nat Rev Earth Environ, v. 4, 149–165 (2023)
5. A. Dini, P. Lattanzi, G. Ruggieri, and E. Trumpy. Lithium occurrence in Italy—An overview, Minerals, v. 12, 945 (2022)
6. Y. Zhao, P. Long, H. Zhang, et al. The occurrence characteristic and dissolution mechanism of lithium-rich sediments in Salt Lake Mahai of Qaidam Basin, NW China, Sci Rep, v. 15, 4291 (2025).
7. J. Yang, H. Wen, C. Luo, Y. Zhang, W. Yu, and C. Zhu. Host minerals of lithium in Jiujialu Formation Li–rich claystones in South China, and implications for the genesis, Journal of Geochemical Exploration, v. 278, 107865 (2025)
8. Z. Wu, X. Hao, and H. Cheng. The occurrence and characterization of lithium in different lithium-bearing clay minerals from bauxite sequences, Gondwana Research, v. 152, 259-271 (2026)
9. W. Li, and X.-M. Liu. Mineralogy and fluid chemistry controls on lithium isotope fractionation during clay adsorption, Science of The Total Environment, v. 851, Pt. 1, 158138 (2022)
10. P. Tien, P. B. Leavens, E. B. Nuhfer. Swinefordite, a new dioctahedral-trioctahedral Li-rich member of the smectite group, American Mineralogist, v. 60, p. 540–547 (1975)
11. C. Ma, and R.A. Eggleton. Surface Layer Types of Kaolinite: A High-Resolution Transmission Electron Microscope Study, Clays and Clay Minerals, v. 47, no. 2, 181–191 (1999)
12. C.A.J. Appelo, and D. Postma. Geochemistry, Groundwater and Pollution, 2nd Edition, A.A. Balkema Publishers, Leiden, 649 pp (2005)
13. F.S. Vinhado, P. Taylor, and S.G. Anderson. Lithium Extraction from Clay Minerals—A Review, Minerals, v. 12, no. 10, 1297 (2022)
14. K. Ling, H. Wen, and Z. Zhang. Distribution and Occurrence State of Lithium in Carbonate-hosted Clay-type Lithium Deposits in the Pingguo Area, Guangxi, South China, Journal of Geochemical Exploration, v. 224, 106757 (2021)
15. S. Al-Ofi, S. Ma, and G. Jin. Resolving Challenges in Analysing Iron-Rich Samples by X-Ray Diffraction, The 36th International Symp of the Society of Core Analysts, Abu Dhabi, 9-12 Oct (2023)
16. W. Guo, S. Ma, and J. Kharrazi. Petrography-guided mineral identification and quantification- user perspectives based on a multi-lab comparative study of XRD, XRF, and FTIR, The 39th International Symp of the Society of Core Analysts, Mexico City, Mexico, 17-21 Aug (2026)
17. A. Alkhaldi, T. Okasha, and S. Ma. Measurement of cation exchange capacity -a lab comparative study, SPE-227122, MEOSGEO, 16-18 Sept (2025)
18. G. Jiang. Effect of Gas Wettability on the Surface Properties of Rocks, in G. Jiang, ed., Gas Wettability of Reservoir Rock Surfaces with Porous Media, Gulf Professional Publishing, p. 121–162 (2018)
19. S. Ma and M. Amabeoku. Core analysis with emphasis on carbonate rocks- quality assurance and control for accuracy & representativeness, *Journal of Interpretation*, Feb, (2015)
20. Ž. Zgorelec, B. Grahovac, A. Perčin, et al. Comparison of Two Different CEC Determination Methods Regarding the Soil Properties, Agriculturae Conspectus Scientificus, v. 84(2), p. 151–158 (2019)
21. D. Jaremko, and D. Kalembasa. A Comparison of Methods for the Determination of Cation Exchange Capacity of Soils, Ecological Chemistry and Engineering S, v. 21, no. 3, 487–498 (2014)
22. C. Ma, R. A. Eggleton. Cation Exchange Capacity of Kaolinite, Clays and Clay Minerals, v. 47, p. 174–180 (1999)
23. M. D. Foster. The Relation Between Illite, Beidellite, and Montmorillonite, Clays and Clay Minerals, v. 2, p. 386–397 (1953)

24. Y. Dehmani, I. Bentahar, H. Lgaz, et al.. A critical review of natural clay minerals: structural characterization, textural properties, and adsorption mechanisms for sustainable wastewater treatment, Materials Today Advances, v. 29, 100682 (2026)

25. Q. Li, X. Liu, K. Wang, C. Cheng, Z. Yin, R. Wang, X. Lu. Revealing atomistic mechanism of lithium diffusion in montmorillonite structure: a molecular simulation study, Geochimica et Cosmochimica Acta, v. 392, p. 165–174 (2025)

26. S. Yenisoy-Karakaş. Uncertainty assessment including sampling for ICP-OES environmental analysis, Journal of Chemical Metrology, v. 1, p. 10–24 (2007)